

Formation of localized hole states in complex oxides

H. Donnerberg, S. Többen, A. Birkholz
University of Osnabrück, FB Physik, D-49069 Osnabrück, FRG
(May 7, 2017)

Defect electrons (holes) play an important role in most technologically important complex oxides. In this contribution we present the first detailed characterization of localized hole states in such materials. Our investigations employ advanced embedded-cluster calculations which consistently include electron correlations and defect-induced lattice relaxations. This is necessary in order to account for the variety of possible hole-state manifestations.

PACS numbers: 71.55Ht, 71.50.+t

I. INTRODUCTION

The basic structural building units of solid oxides are MO_6 metal-oxygen octahedra and, possibly, additional MO_4 tetrahedra. The complete crystal structure is built up of corner-, face- and/or edge-sharing connections of these structural elements. Additional cations (A) can be incorporated at interstitial lattice sites. These are increasingly formed, the more open-structured the whole network of MO_n units appears to be. Generally, open crystal structures imply high formal M-cation charge states (referring to formal O^{2-} anions) leading to mixed ionic-covalent (or semi-ionic) material properties. The M-cations are in most cases transition-metal (TM) ions. Examples of such complex materials are given by AMO_3 perovskite-structured oxides such as barium titanate (BaTiO_3). Perovskite oxides are frequently ferroelectric and possess important electrooptic applications based on the photorefractive effect. Also high- T_C oxides resemble the perovskite structure.

Charge carriers, either valence-band (VB) holes or conduction-band (CB) electrons, are created by doping with impurities, annealing treatments or by light-induced charge-transfer excitations which, for example, take place during photorefractive processes in the appropriate oxides. Combined optical-absorption- and electron-spin-resonance measurements (Photo-ESR) [1] proved that the created and afterwards trapped holes influence the light-induced charge-transfer reactions in photorefractive BaTiO_3 . These holes, which are either para- or diamagnetic, probably induce the observed sublinear dependence of photoconductivity on the light intensity (e.g. [2]). A further example highlighting the relevance of holes refers to high- T_C oxides: Pairs of doped holes give rise to superconductivity in these materials. The possible pairing scenarios are still a matter of active debate.

The present work initiates a systematic and detailed characterization of localized hole states in complex oxides. Our investigations employ real-space embedded-cluster calculations, which consistently combine electron correlations and defect-induced lattice relaxations. This procedure is indispensable in order to predict the richness of possible hole states. Here, we demonstrate simulations for trapped holes in BaTiO_3 , but many results, ranging from stabilization of cationic charge states to the formation of bipolarons, can be extrapolated to other oxides.

The trapping of holes at acceptor defects leads to a localization of hole states, which is further aided by defect-induced lattice distortions. In near-insulating high- T_C oxides the antiferromagnetic order supports hole localizations. Principally, there is 'on-acceptor' and 'off-acceptor' hole trapping. In the first case the trapped hole localizes at the acceptor site (thereby increasing the acceptor charge state by one positive unit, i.e. $\text{M}^{+n} + \text{h}^\bullet \rightarrow \text{M}^{+(n+1)}$), and in the second case the hole remains at the oxygen ligands. Further, the off-acceptor case allows to classify hole states according to their degree of delocalization, i.e. complete localization at exactly one ligand anion, intermediate localization at two neighboring oxygen ions (V_k centers), and delocalization over more than two oxygen ligands.

Which hole-localization type is favored depends on the ionicity of the host system, but also on the incorporation site and electronic structure of the acceptor. For example, at Ba-site acceptors localized off-acceptor holes are likely to be preferred over delocalized species due to large interionic separations [3]. Further, the simultaneous binding of two holes at one acceptor facilitates the formation of small intersite bipolarons representing negative- U centers. Such species could explain the diamagnetic hole centers in photorefractive oxides [1]; intersite bipolarons have also been considered as possible superconductivity-carrying bosons in high- T_C oxides (see [4], for details). Earlier work on bipolarons in oxide materials dealt exclusively with electron type species. We quote in this context the pioneering work of P. W. Anderson [5] on the formation of negative- U centers in amorphous solids. Schlenker [6] investigated small electron type bipolarons in titanium oxides.

II. METHODS

Our investigations employ real-space embedded-cluster calculations (ECC), in which the crystal is divided into a central and quantum chemically treated defect cluster and into the embedding lattice which is modeled more approximately. The ECC discussed in this publication deal with the trapping of holes at Ti-site acceptors in BaTiO₃. Our calculations are based on 21-atom clusters MO₆Ba₈Ti₆ centered around an acceptor-oxygen octahedron MO₆, see also [7]. All simulations assume the perfect-crystal structure of cubic BaTiO₃. This simplification may be justified due to the observation that all possible ferroelectric distortions of the material are small compared with usual defect-induced lattice relaxations.

The molecular-orbital ansatz for the central MO₆ complex employs Gaussian type basis functions with split-valence quality for the acceptor metal impurity and its oxygen ligands; the oxygen basis set is further augmented by polarizing *d*-functions. Bare effective core potentials [8] are used to model the localizing ion-size effects of the outer Ba- and Ti-cations. The *ab initio* level of our calculations covers Hartree-Fock (HF) theory, Møller-Plesset perturbation theory to second order (MP2) and density functional theory (DFT). All quantum cluster simulations have been performed on the basis of the quantum-chemical CADPAC code [9]. Within DFT two choices are used to approximate the exchange-correlation functional, i.e. the local spin density ansatz of Vosko, Wilk and Nusair [10] (VWN-LSDA) and the generalized-gradient-approximation functional involving the Becke exchange term [11] and the correlation functional derived by Lee, Yang and Parr [12]. This functional, abbreviated as 'BLYP', improves on LDA.

The modeling of the embedding lattice and of cluster-lattice interactions employs a shell-model pair-potential description (see also Refs. [7,13,14]). The shell-model parameters have been taken from the earlier work of Lewis and Catlow [15]. It is noted that the shell model takes electronic polarization contributions of the embedding lattice ions reasonably well into account. This feature is particularly important with respect to the highly polarizable oxygen anions. Figure 1 displays the embedding scheme. As in any classical Mott-Littleton defect calculation the (embedding)

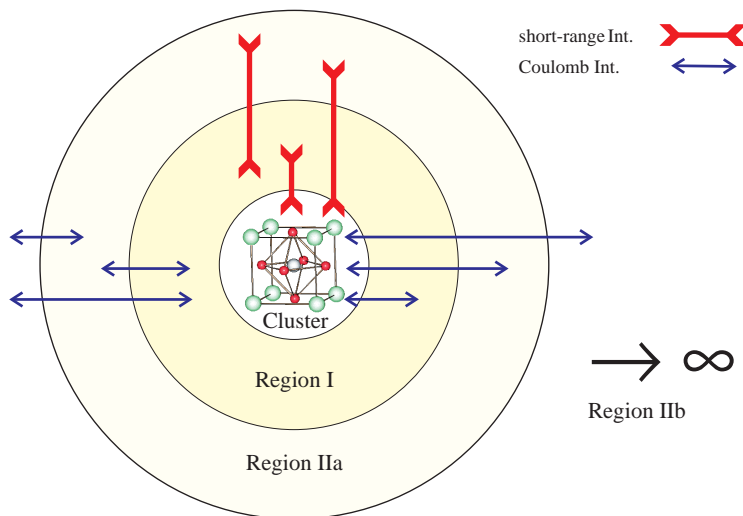


FIG. 1. Visualization of embedded-cluster calculations. The quantum cluster is embedded in a classically treated lattice consisting of the regions I, IIa and IIb. The arrows indicate the various existing interactions between the crystal regions.

crystal lattice is divided into three regions: region I which is explicitly equilibrated according to the underlying pair potentials, the interface region IIa and region IIb. Region II(a and b) is treated as a polarizable continuum using the harmonic approximation for the region-II self-energy. Whereas the interactions between the cluster and region I, on the one hand, and region IIa, on the other hand, are included explicitly, all region-IIb species feel only the effective defect charge of the central defect cluster. Details of this well-known description are given in Ref. [16]. All lattice calculations employ the CASCADE code [17].

The total energy of the complete model crystal is given by the expression:

$$E(\rho, R_c, R_r) = \min_{\rho, R_c, R_r} \{E_{\text{Clust}}^{\text{QM}}(\rho, R_c) + E_{\text{Env}}^{\text{SM}}(R_r) + E^{\text{Int}}(\rho, R_c, R_r)\}. \quad (1)$$

ρ , R_c and R_r denote the cluster electron density, the coordinates of the cluster nuclei and the positions of the shell-model species in the embedding environment, respectively. $E_{\text{Clust}}^{\text{QM}}$ represents the quantum mechanically calculated cluster self-energy, $E_{\text{Env}}^{\text{SM}}$ the Mott-Littleton type shell-model energy of the embedding environment and E^{Int} is the cluster-lattice interaction energy. The required minimization in Eq.(1) is performed using the programs CADPAC (variation of ρ with fixed R_r) and CASCADE (variation of R_r with fixed R_c and ρ). In order to do cluster geometry optimizations which are consistent with a predetermined embedding crystal lattice (represented by a point-charge field) an additional program has been written which updates the total cluster energies and gradients, as calculated by any quantum chemical program such as CADPAC, by adding the appropriate short-range pair-potential contributions due to the interactions between cluster ions and embedding lattice species. With these updates the program carries through the cluster geometry optimization using a variable-metric (quasi-Newton) minimization algorithm. The total minimization procedure is completed, when the main cycle consisting of the alternating lattice- and cluster-equilibration subcycles converges. It is finally noted, that we have neglected the full cluster multipole consistency during the embedding-lattice relaxation step (see [18], for details), since, in our simulations, we did not observe any appreciable relaxation and energy changes due to cluster multipole contributions deviating from formal-charge models.

The present approach proves to be the only successful one which can consistently integrate the local electronic structure and large-scale lattice-distortion effects. In particular, we find the combination of DFT and of our embedding scheme to be sufficiently accurate and flexible in order to realistically account for the variety of possible hole states. We stress that cutting off the electronic structure beyond the cluster boundary does not principally invalidate our results. This is due to the fact that embedded-cluster calculations formally refer to a localized-orbital point of view (e.g. see [19,7] for related discussions) and not to the extended one-electron eigenstates of the crystal. Moreover, all hole states considered in this contribution may be assumed to be localized within the cluster region due to the presence of the acceptor defect and due to pronounced lattice deformations (small-polaron effect). Further indications towards a reliability of our present results are provided by our earlier calculations of optical charge-transfer (CT) transitions at transition-metal cations [7], which compare favorably with experimental data. The CT states may be considered as excited states of trapped holes.

III. RESULTS AND DISCUSSION

In the following discussion, in each case we start with the ionic HF model and add on correlations afterwards to demonstrate important implications.

First, we discuss single holes trapped at TM cations. Within HF theory, on-acceptor holes are favorable for divalent TM cations including Cu^{2+} , which possess filled electron levels above the VB edge. At trivalent Ti-site TM acceptors, on the other hand, localized (i.e. symmetry-breaking) off-acceptor holes are highly preferred (Table I). Here, we observe the hole localization in π -type oxygen $2p$ -orbitals (perpendicular to the oxygen-acceptor axis).

TABLE I. Total HF and MP2 embedded-cluster energies for different hole states including lattice relaxations. Energies are renormalized to localized off-acceptor states. $\text{O}_O^-(\pi, \sigma)$: localized off-acceptor hole in oxygen $2p$ π - or σ -type orbitals. $(\text{O}(\text{xy}))^-$: off-acceptor hole delocalized over the four oxygen ligands in the xy -plane. $2S + 1$ denotes the total spin multiplicity of the cluster. Note that Fe^{3+} and Cr^{3+} favor high spin ($2S_{\text{Fe}} + 1 = 6$, $2S_{\text{Cr}} + 1 = 4$), and Rh^{4+} prefers low spin ($2S_{\text{Rh}} + 1 = 2$).

Defect	$2S + 1$	$\Delta E_{\text{total}}^{\text{UHF}}$ (eV)	$\Delta E_{\text{total}}^{\text{MP2}}$ (eV)
$\text{Fe}_{\text{Ti}}^{3+} - \text{O}_O^-(\pi)$	7	0.0	0.0
$\text{Fe}_{\text{Ti}}^{3+} - \text{O}_O^-(\sigma)$	5	0.0	-
$\text{Fe}_{\text{Ti}}^{3+} - \text{O}_O^-(\pi)$	7	+1.1	-
$\text{Fe}_{\text{Ti}}^{3+} - \text{O}_O^-(\sigma)$	5	+1.0	-
$\text{Fe}_{\text{Ti}}^{3+} - (\text{O}(\text{xy}))^-$	7	+2.4	+0.5
$\text{Fe}_{\text{Ti}}^{4+}$	5	+2.4	+0.1
$\text{Rh}_{\text{Ti}}^{3+} - \text{O}_O^-(\pi)$	2	0.0	0.0
$\text{Rh}_{\text{Ti}}^{3+} - (\text{O}(\text{xy}))^-$	2	+2.7	+0.1
$\text{Rh}_{\text{Ti}}^{4+}$	2	+0.4	-2.4
$\text{Cr}_{\text{Ti}}^{3+} - \text{O}_O^-(\pi)$	5	0.0	0.0
$\text{Cr}_{\text{Ti}}^{4+}$	2	+1.15	-2.6

This symmetry-broken state is stabilized by defect-induced lattice distortions and, in this way, it can acquire physical significance. The relaxation-induced energy gain is typically 1 eV, which emphasizes the importance of such terms.

The occurrence of symmetry-broken solutions may be considered as electronic polaron self-trapping. Generally, hole localization in σ -type orbitals (parallel to the oxygen-acceptor axis) is less favorable, but deviations may occur due to the actual electronic acceptor structure.

Interestingly, both delocalized off-acceptor holes and the formation of tetravalent TM ions are unfavorable within HF. For example, delocalized off-acceptor holes are by 2 – 3 eV discriminated against their localized counterparts. Similar results have been obtained in previous HF simulations on trapped single holes in MgO [20,21] and NiO [22]. Also these calculations predict localized off-acceptor holes to be most favorable. In fact such holes are likely the most favorable off-acceptor solutions in highly ionic oxides like MgO, but this behavior may prevail in any HF calculation, thus simulating artificially ionic situations.

In BaTiO₃ the effects of electron correlation are most significant for trivalent TM acceptors due to the increased covalent charge transfer from oxygen onto the TM ions. This has important consequences: The on-acceptor hole localization is enhanced, and, simultaneously, possible off-acceptor holes increasingly delocalize. In contrast, at most divalent TM cations including Cu²⁺ on-acceptor holes remain stable. This behavior differs from La₂CuO₄ where, confirmed by our preliminary ECC, doped holes localize at the oxygen sites. The different *effective* copper charges in both oxides can explain such deviations. Further work on La₂CuO₄ is in progress and will be published in the near future.

Our MP2 calculations (Table I) illustrate that electron correlation tends to favor on-acceptor holes at trivalent TM acceptors. Rh⁴⁺ and Cr⁴⁺ become preferred over M – O⁻ centers, but Fe⁴⁺ remains 0.1 eV less favorable than Fe³⁺ – O⁻. Within DFT even Fe⁴⁺ is stable, and for all trivalent TM acceptors the most favorable off-acceptor holes are delocalized at this level.

Considering off-acceptor holes, correlation mostly affects the delocalized hole states, but localized states to a much lesser extent. These off-acceptor-hole results demonstrate the pronounced interplay between orbital relaxations and electron correlation, i.e. the localized hole states with significant HF orbital relaxations receive less correlation-energy gain than delocalized hole states. However, different from HF theory the energy separations between localized and delocalized off-acceptor holes remain within some tenths eV. This result indicates that a modest increase of ionicity could favor localized over delocalized off-acceptor holes. The lanthanide contraction of 5*d* TM cations might accomplish such changes leading to observable localized off-acceptor holes, if these are sufficiently stable against the formation of on-acceptor holes. ESR data suggest that localized off-acceptor holes bound to ESR-silent Pt-acceptors exist in BaTiO₃ [3]. The charge state of platinum could not be assessed experimentally, but Pt⁴⁺ with a completely filled 5*d*(*t*_{2*g*}) subshell is a possible candidate.

In summary, electron correlation essentially stabilizes the high-valent charge states of various TM cations in BaTiO₃. This mechanism resembles the Haldane-Anderson scenario [23] in semiconductors. In highly ionic materials, in contrast, the charge-state stabilization has been ascribed to lattice relaxations [24]. The present discussion confirms that BaTiO₃ is semi-ionic.

In comparison to most TM acceptors the hole localization properties can differ at ionic acceptor cations due to the lack of filled acceptor levels above the VB edge and of covalent charge transfer. Table II exemplifies the situation for Al³⁺. Obviously, on-acceptor hole states leading to Al⁴⁺ are highly unfavorable. ESR investigations furnished

TABLE II. Hole formations at Al_{Ti}³⁺. Total embedded-cluster energies are renormalized to the localized off-acceptor π -type hole state. The results include lattice relaxation.

Defect	$\Delta E_{\text{total}}^{\text{UHF}}$ (eV)	$\Delta E_{\text{total}}^{\text{MP2}}$ (eV)	$\Delta E_{\text{total}}^{\text{BLYP}}$ (eV)
Al _{Ti} ³⁺ – O _O ⁻ (π)	0.0	0.0	0.0
Al _{Ti} ³⁺ – (deloc. (π)) ⁻	+2.5	+0.4	-0.8
Al _{Ti} ³⁺ – (deloc. (σ)) ⁻	+3.7	+1.9	-
Al _{Ti} ³⁺ – (V _k (π))	+1.0	0.0	-0.4
Al _{Ti} ³⁺ – (V _k (σ))	+2.8	+1.6	-

evidence in favor of V_k hole centers (i.e. one hole delocalized over two neighboring ligands) [25], but there are no such indications for other acceptors in BaTiO₃.

As expected, HF favors localized off-acceptor π -type holes. Next favored is the V_k π -type hole distribution (Fig.2), but it is by 1 eV less favorable. The situation is even worse for completely delocalized states. Again electron correlation supports hole delocalization. The correlated calculations reported in Table II confirm that all hole states are of comparable energy. Most favorable are the delocalized state and the formation of V_k centers. However, there is no clear indication in favor of the latter species. But the results suggest a delicate balance between the local electronic structure and defect-induced lattice distortions: Increasing the acceptor ionicity would lead to localized off-acceptor

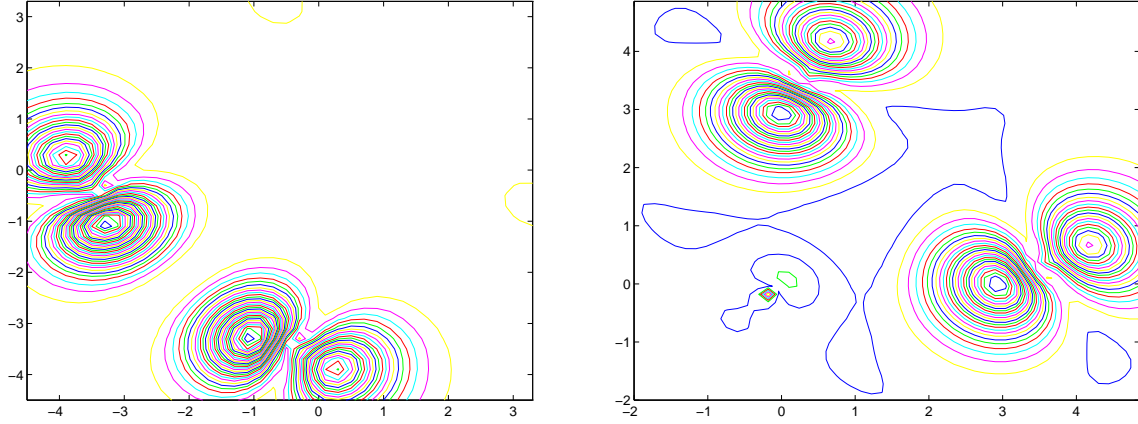


FIG. 2. Hole spin density plot of π - and σ -type V_k centers trapped at $\text{Al}_{\text{Ti}}^{3+}$. The occupation of oxygen $2p$ orbitals can be clearly seen. The acceptor is at $(x,y)=(0,0)$ in both cases. All xy -coordinates in the figures are given in atomic units. The interatomic separation between the oxygen partners forming the V_k defect is 2.3 \AA and 2.6 \AA for localization in π - and σ -type oxygen orbitals, respectively. The perfect-lattice separation is 2.8 \AA .

holes, whereas a reduced ionicity implies hole delocalization. In an intermediate small 'window' the formation of V_k centers might be most favorable. This also explains why V_k centers are rarely observed in oxides. Experimentally the Al-cation fits into this window, but also the present embedded-cluster model is close to this situation. Interestingly, V_k centers have been also proposed in Al_2O_3 [26].

Due to reduced bonding σ -type V_k centers are by 1.6 - 1.8 eV less favorable than π -type ones. All ion displacements are smaller in the σ -type modification. We stress that these results refer to Al^{3+} acceptors, but it is recalled that holes doped into the Cu-O planes of high- T_C oxides are assumed to populate σ -type oxygen orbitals [27], which, following our preliminary calculations, is related to the occupation of copper $3d_{x^2-y^2}$ states and to the presence of strong electron correlations. Our present results receive particular importance, since V_k centers (upon addition of a second hole) bear resemblance to small intersite hole bipolarons. Thus, we may expect the same relaxation behavior for hypothetical π -type and σ -type hole bipolarons in high- T_C oxides. Due to moderate lattice distortions the latter species would be more appropriate to coherent motions. Speculatively, σ -type bipolarons could facilitate superconductivity, thereby supporting the scenario of Alexandrov and Mott [4]. Certainly, our speculations deserve further detailed investigations.

We finally review trapped hole bipolarons in BaTiO_3 ; the details of the calculations are discussed extensively in Refs. [13,14]. Ti-site Mg^{2+} is considered as the actual acceptor cation. Two geometrical hole-acceptor configurations are compared: the bipolaron with two holes on neighboring oxygen ions (i.e. literally a V_k center with one additional hole) and a linear complex $\text{O}^- - \text{Mg}_{\text{Ti}}^{2+} - \text{O}^-$. The presence of two holes introduces a natural driving force towards localization, of which the linear complex corresponds to minimizing the inter-hole Coulomb repulsion. Both hole complexes have been studied under different conditions: (1) HF treatment of the cluster employing a rigid and perfectly structured crystal lattice. Only the actual O^- partners are allowed to relax. (2) HF description of the cluster including lattice relaxation. (3) Correlated calculations (MP2 and DFT). To save computer capacities further geometry optimizations have been performed at the DFT level (LSDA and BLYP) only.

We first survey the perfect-lattice HF simulations. Electronic interactions between the O^- ions and nearby crystal ions favor the spin triplet over the singlet state. Due to its antisymmetrical charge distribution the triplet-state bipolaron benefits most from this interaction. Increasing the bipolaron bond length rapidly disturbs the bipolaron type states due to hole-state delocalizations. But energetically most favorable is the linear complex. This expected result reflects the disfavor of delocalized holes within HF. The linear configuration with either spin is 1 eV more favorable than the triplet-state bipolaron.

Next we consider the effect of lattice deformations. Most importantly, our ECC demonstrate that defect-induced lattice relaxation and electronic correlations stabilize hole bipolarons in BaTiO_3 . Lattice relaxations increase the localization of bipolaron states and favor the spin-singlet state. Thus, such relaxations enable the possibility of embedded O_2^{2-} molecules analogous to isoelectronic F_2 dimers. Noticeably, both species are unstable within HF (e.g. see [14]). The ultimate stability is established by correlation-induced bonding terms. Binding energies of bipolarons can be estimated as the energy difference $E(\text{BP}) - E(\text{O}^- - \text{Mg} - \text{O}^-)$, since, due to shell-model estimates, the

competitive linear complex is only weakly bound in BaTiO₃. We obtain -0.41 eV (MP2), -1.13 eV (DFT-BLYP) and -2.1 eV (DFT-LSDA). Calculated bond lengths are: 1.48 Å (LSDA) and 1.55 Å (BLYP). As is frequently observed [28], LSDA overestimates bonding. The accurate binding energy is enclosed by the BLYP- and MP2 values.

We believe that paired holes are of general importance in any oxide. Possible differences will refer to the occupation of π - or σ -type oxygen $2p$ orbitals giving different bonding strengths. Finally, we emphasize that the singlet-triplet splitting of bipolaron states, i.e. the 'spin gap', depends on the strength of lattice relaxations. Whereas in perfect lattices the triplet state is preferred, the singlet state becomes most favorable upon lattice distortions. For π -type bipolarons in BaTiO₃, due to our MP2 calculations, the spin gap becomes 1.50 eV in this case. We note that this value is essentially intrinsic to the hole bipolarons in BaTiO₃, and does not depend on the specific nature of the magnesium acceptor ion. In particular, the bipolaron states are not contaminated by magnesium orbitals; we, therefore, expect a similar spin gap for possibly existing isolated bipolarons in BaTiO₃. In their bipolaron theory of high- T_C superconductivity Mott and Alexandrov suggested a spin gap of a few tens meV [4]. Such a small value would indicate that, compared with BaTiO₃, lattice relaxations are present but less developed in high- T_C oxides. This observation is important if coherent motion of bipolarons is to be required.

ACKNOWLEDGMENTS

We gratefully acknowledge the financial support of this work by the Deutsche Forschungsgemeinschaft (SFB 225). We also thank Prof. O. F. Schirmer and Prof. M. Wöhlecke for many valuable discussions.

-
- [1] E. Possenriede, P. Jacobs, H. Kröse, and O. F. Schirmer. *Appl. Phys.* **A55**, 73 (1992).
 - [2] L. Holtmann. *phys. stat. sol. (a)* **113**, K 89 (1989).
 - [3] T. Varnhorst, O. F. Schirmer, H. Kröse, R. Scharfschwerdt, and Th. W. Kool. *Phys. Rev.* **B53**, 116 (1996).
 - [4] A. S. Alexandrov and N. F. Mott. *Rep. Prog. Phys.* **57**, 1197 (1994).
 - [5] P. W. Anderson. *Phys. Rev. Lett.* **34**, 953 (1975).
 - [6] C. Schlenker. In D. Adler, H. Fritzsche, and S. R. Ovshinsky, editors, *Physics of Disordered Materials: Mott Festschrift*, volume 3. Plenum Press, New York, 1985.
 - [7] H. Donnerberg and R. H. Bartram. *J. Phys.: Condens. Matter* **8**, 1687 (1996).
 - [8] W. R. Hay and P. J. Wadt. *J. Chem. Phys.* **82**, 270–310 (1985).
 - [9] R. D. Amos and et al., 1994. Cambridge Analytic Derivatives Package (CADPAC) version 5.2 (Cambridge).
 - [10] S. H. Vosko, L. Wilk, and M. Nusair. *Can. J. Phys.* **58**, 1200 (1980).
 - [11] A. D. Becke. *Phys. Rev.* **A38**, 3098 (1988).
 - [12] C. Lee, W. Yang, and R. G. Parr. *Phys. Rev.* **B37**, 785 (1988).
 - [13] H. Donnerberg and A. Birkholz. *J. Phys.: Condens. Matter* **7**, 327 (1995).
 - [14] H. Donnerberg. *J. Phys.: Condens. Matter* **7**, L689 (1995).
 - [15] G. V. Lewis and C. R. A. Catlow. *J. Phys. Chem. Solids* **47**, 89 (1986).
 - [16] C. R. A. Catlow and W. C. Mackrodt, editors. *Computer Simulation of Solids*, volume 166 of *Lecture Notes in Physics*. Springer Verlag, Berlin, Heidelberg, New York, 1982.
 - [17] M. Leslie. *Solid State Ionics* **8**, 243 (1983).
 - [18] J. M. Vail, A. H. Harker, J. H. Harding, and P. Saul. *J. Phys. C: Solid State Phys.* **17**, 3401 (1984).
 - [19] A. B. Kunz and D. L. Klein. *Phys. Rev.* **B17**, 4614 (1978).
 - [20] A. L. Shluger, E. A. Kotomin, and L. N. Kantorovich. *J. Phys. C: Solid State Phys.* **19**, 4183 (1986).
 - [21] A. L. Shluger, E. N. Heifets, J. D. Gale, and C. R. A. Catlow. *J. Phys.: Condens. Matter* **4**, 5711 (1992).
 - [22] J. Meng, P. Jena, and J. M. Vail. *J. Phys.: Condens. Matter* **2**, 10371 (1990).
 - [23] F. D. M. Haldane and P. W. Anderson. *Phys. Rev.* **B13**, 2553 (1976).
 - [24] A. M. Stoneham and M. J. L. Sangster. *Phil. Mag.* **B43**, 609 (1981).
 - [25] E. Possenriede, P. Jacobs, and O. F. Schirmer. *J. Phys.: Condens. Matter* **4**, 4719 (1992).
 - [26] L. Kantorovich, A. Stashans, E. Kotomin, and P. W. M. Jacobs. *Int. J. Quant. Chem.* **52**, 1177 (1994).
 - [27] J. Fink, N. Nücker, H. A. Romberg, and J. C. Fuggle. *IBM J. Res. Develop.* **33**, 372 (1989).
 - [28] P. Fulde. *Electron Correlations in Molecules and Solids*, volume 100 of *Solid-State Sciences*. Springer Verlag, Berlin, Heidelberg, 1991.